NBSIR 76-1141

Study of Initial Stages of Wear by Electron Channeling

I. Measurement of Plastic Strain in Copper Due to Sliding Wear

II. Quantitative Methods in Wear Debris Analysis

A. W. Ruff

Institute for Materials Research
National Bureau of Standards
Washington, D. C. 20234

September 1976

Final Report

NOOO 14-76-F-002

Prepared for
Office of Naval Research
Department of the Navy
Arlington, Virginia 22217

NBSIR 76-1141

STUDY OF INITIAL STAGES OF WEAR BY ELECTRON CHANNELING

I. Measurement of Plastic Strain in Cooper Due to Sliding Wear

II. Quantitative Methods in Wear Debris Analysis

A. W. Ruff

Institute for Materials Research
National Bureau of Standards
Washington, D. C. 20234

September 1976

Final Report

NOOO 14-76-F-002

Prepared for
Office of Naval Research
Department of the Navy
Arlington, Virginia 22217

U.S. DEPARTMENT OF COMMERCE, Elliot L. Richardson, *Secretary*

Edward O. Vetter, *Under Secretary*

Dr. Betsy Ancker-Johnson, *Assistant Secretary for Science and Technology*

NATIONAL BUREAU OF STANDARDS, Ernest Ambler, *Acting Director*

SECURITY CLASSIFICATION OF THIS PAGE *(When Data Entered)*

REPORT DOCUMENTATION PAGE

READ INSTRUCTIONS BEFORE COMPLETING FORM

1. REPORT NUMBER: NBSIR 76 -1141	2. GOVT ACCESSION NO.
3. RECIPIENT'S CATALOG NUMBER	
4. TITLE *(and Subtitle)*: Study of Initial Stages of Wear by Electron Channeling	5. TYPE OF REPORT & PERIOD COVERED: Final Report
6. PERFORMING ORG. REPORT NUMBER	
7. AUTHOR*(s)*: A. W. Ruff	8. CONTRACT OR GRANT NUMBER*(s)*: NOOO 14-76-F-002
9. PERFORMING ORGANIZATION NAME AND ADDRESS: A. W. Ruff, National Bureau of Standards, Washington, D.C. 20234	10. PROGRAM ELEMENT, PROJECT, TASK AREA & WORK UNIT NUMBERS
11. CONTROLLING OFFICE NAME AND ADDRESS: Dept. of the Navy, Office of Naval Research--ATTN: R. S. Miller, Arlington, VA 22217	12. REPORT DATE: September 1976
	13. NUMBER OF PAGES
14. MONITORING AGENCY NAME & ADDRESS*(If different from Controlling Office)*	15. SECURITY CLASS. *(of this report)*: Unclassified
	15a. DECLASSIFICATION/DOWNGRADING SCHEDULE

16. DISTRIBUTION STATEMENT *(of this Report)*

Distribution of this document is unlimited

17. DISTRIBUTION STATEMENT *(of the abstract entered in Block 20, if different from Report)*

18. SUPPLEMENTARY NOTES

19. KEY WORDS *(Continue on reverse side if necessary and identify by block number)*

Copper; electron channeling; electron microscope; metals; particle analysis; plastic deformation; surfaces; wear; wear debris; x-ray analysis.

20. ABSTRACT *(Continue on reverse side if necessary and identify by block number)*

Wear experiments have been conducted to determine the plastic strains that are troduced in the surface material near sliding wear tracks. Both oil lubricated and y sliding experiments have been carried out at different sliding distances on surces of copper. The strain values were determined from selected area electron channelg patterns obtained using a scanning electron microscope from regions as small as μm in size and 0.05 μm deep around the wear track. A deformed calibration specimen

DD FORM 1 JAN 73 1473 EDITION OF 1 NOV 65 IS OBSOLETE
S/N 0102-014-6601

SECURITY CLASSIFICATION OF THIS PAGE *(When Data Entered)*

was used to relate electron channeling band contrast to deformation strain. Strain maps were obtained on the wear surface lateral to the wear track and also below the surface using electropolishing metal removal techniques. Particular attention was placed on the near-surface strain values. In all cases, the maximum strain was found at the wear surface located at the track center and the strains decreased uniformly with depth. Significant, large strains were also found outside the wear tracks. The results are compared with those previously reported for iron and with recent theoretical models.

Wear debris has been removed from a number of test systems and analyzed using different methods. Those methods produced specific information concerning the particulate size and composition. A magnetic debris recovery method was quantitatively evaluated using actual debris samples and also using collections of manufactured particulates having known sizes and compositions. Small 5 μm diameter SiO_2 spheres, some containing nickel, were used to simulate debris. Other particulates of iron and nickel in different size ranges were also used in order to investigate such matters as size resolution, lubricant dilution techniques, particle overlap difficulties, and the general problem of calibration of debris recovery systems. A comparison between chemical analysis and particulate analysis findings is presented. The application of optical and electron microscope methods and x-ray microanalysis in characterizing the wear particulates was carried out directly on the recovery substrate; those techniques are described.

Measurement of Plastic Strain in Copper Due to Sliding Wear

A. W. Ruff
Metallurgy Division
National Bureau of Standards
Washington, D.C. 20234

ABSTRACT

Wear experiments have been conducted to determine the plastic strains that are introduced in the surface material near sliding wear tracks. Both oil lubricated and dry sliding experiments have been carried out at different sliding distances on surfaces of copper. The strain values were determined from selected area electron channeling patterns obtained using a scanning electron microscope from regions as small as 10 μm in size and 0.05 μm deep around the wear track. A deformed calibration specimen was used to relate electron channeling band contrast to deformation strain. Strain maps were obtained on the wear surface lateral to the wear track and also below the surface using electropolishing metal removal techniques. Particular attention was placed on the near-surface strain values. In all cases, the maximum strain was found at the wear surface located at the track center and the strains decreased uniformly with depth. Significant, large strains were also found outside the wear tracks. The results are compared with those previously reported for iron and with recent theoretical models.

INTRODUCTION

Investigations into the mechanisms of the wear of materials are of crucial importance if significant progress is to be made in reducing wear or even in monitoring wear rates. The analysis of wear debris recovered from lubricants and wearing systems has proven (1-3) to offer valuable information on the condition of such systems, however, the significance of debris analysis (if purely empirical methods are to be exceeded) rests on an understanding of debris formation mechanisms. Recent years have seen several important contributions (4,5). In particular, the delamination theory of wear (6) postulates a wear particle formation process that appears to agree with certain observations. That approach incorporates certain material parameters in the model used and recognizes the influence of imperfections, e.g. voids, inclusions and the free surface. One unusual aspect of that model involves surface softening, i.e.,

dislocation density and flow stress gradients such that both quantities increase initially with distance inward from the surface. That circumstance develops according to this picture as a result of surface image forces on the dislocations produced during the wear deformation that lead to a local loss of dislocations as a result of glide out of the surface. Some experimental evidence in copper and aluminum has been cited (7) to support this idea although recent measurements on iron (8) have not found any evidence for the surface softening that would be expected. This paper presents some results obtained on high purity copper specimens tested in sliding wear that also indicates an absence of any surface softening effects. However, it is important to note that this aspect of the delamination model is not crucial (in our view), Indeed the factors responsible for subsurface crack formation and propogation are probably complex and numerous. Data such as those presented here concerning the strain distribution in the material near wear tracks are required if an accurate understanding of the inhomogeneous deformation processes involved in such matters are to be understood.

EXPERIMENTAL

The constant velocity, sliding wear tester used in these studies has been described previously (8). A motor driven cam transmitted a reciprocating velocity (2.0 cm/s) to a platform on which the test specimen was fastened. The linear motion was adjustable up to 2 cm. A load was applied through a pin from above the specimen. A bearing ball of 2.4 mm diameter (52100 steel) was fastened at the end of this pin. The frictional force at the contact surface could be measured during the wear test using strain gauges. Tests of durations from 5 to 500 cycles were conducted under either dry or oil lubricated conditions.

Specimens were fabricated from 99.999% copper sheet, 0.5 mm thick (impurity content 10 ppm C, 5 ppm Zn, others <1 ppm). Specimens were cut to size 1 cm x 2.5 cm and then annealed for 2 hours at 1000°C in an evacuated, sealed quartz tube. Prior to wear testing each specimen was electropolished about 20 minutes in a solution of 67% phosphoric acid:33% water. In experiments involving strain measurements below the worn surface, the same electropolishing procedure was followed in order to remove material in a strain-free manner. An approximate depth of 10 μm of copper was removed from each side of the sheet in 24 minutes.

Specimens were clamped down around the edges within the specimen tray in the wear tester. In tests involving oil lubrication, the specimen tray was filled with SAE 30 weight automotive oil prior to testing. The oil had been previously filtered through a 1.2 μm filter to remove solid impurities. Tests were conducted by mounting the electropolished specimen in the tray, adding oil if desired, loading the pin to the desired value, starting the drive motor and carefully lowering the pin into contact with the specimen. The wear specimen and bearing ball were examined after each test (after cleaning with a solvent) using optical microscopy and scanning electron microscopy (SEM) techniques. The SEM had been modified for selected area electron channeling pattern (SACP) studies involving the rocking beam mode (9,10) of operation. The specimen was oriented normal to the electron beam and operated in the emissive (secondary and backscattered electron) mode. The minimum selected area realizable was about 10 μm across (approximately circular) at a specimen-lens distance of 2 mm. The angular extent of the SACP was about 15 degrees. The microscope was operated at 20 kV and a specimen current of 2×10^{-7} amperes.

RESULTS AND DISCUSSION

Selected Area Channeling Patterns

Previous workers (9-11) have used either the line width or the contrast associated with a particular channeling line as a measure of the strains present in the channeling volume. Channeling lines of different hkl indices (corresponding to the hkl of the planes involved in the channeling process) exhibit different line broadening amounts; the higher index lines are more sensitive to lattice strain. Hence it is necessary to systematically employ the same {hkl} channeling line and to calibrate the effect of strain on that line using a suitably deformed specimen. In this study, the 111 channeling line in copper was used. The contrast of the line was determined according to the relation $C = \{I(max) - I(min)\}/I(avg)$ where I is the detected (amplified) signal level. The method of use of the gain and DC level controls on the SEM that permited quantitative contrast values to be determined from photographs of the signal trace on the recording screen has been described (8). An example of an SACP taken from one grain in an undeformed copper specimen is shown in Fig. 1. The 111 band is labeled and higher order channeling lines are clearly visible as the fine structure in this pattern.

Strain Calibration Specimen

A copper rod, 4.5 mm in diameter, was cut to a length 12.5 mm. Two flat surfaces were ground on opposite sides, one parallel to the rod axis, the other at an angle of about 1.2° to the axis. This resulted in a tapered specimen, 1.35 mm thick at one end and 1.62 mm thick at the other end. The specimen was then electropolished, sealed in an evacuated capsule and annealed for 2 hours at 980°C. The specimen was deformed in compression between two steel plates on which teflon films had been placed until a uniform thickness was reached. In this manner, a gradient in applied true strain from zero to 27% was produced.

SACP from two different regions of the calibration specimen are presented in Fig. 2. Superimposed on these patterns are four signal traces from different regions of the pattern and the two reference signals (white and black levels) that are used in determining the average contrast. Reproducible contrast values were obtained using this method of signal presentation and measurement over the contrast range of 0 to 10%, provided that each specimen was mounted carefully in the SEM in a reproducible manner. A strain determination could be completed at a given location in a matter of minutes using this method.

A sufficient number of grains with 111 channeling bands prominent in their patterns were located and the contrast gradient that resulted from the introduced strain gradient mapped out along the length of the calibration specimen. The results of SACP contrast measurements are given in Fig. 3. Contrast values below 1% were not measured due to poor precision. Strains greater than about 27% in copper cannot reliably be determined by this method. Previous studies of stainless steel (9,10) have shown that strains in excess of about 20% (tensile) could not be reliably measured using SACP methods. In iron (8) strains greater than about 17% (compressive) could not be determined by this method.

Sliding Wear Experiments

Studies were conducted using progressively larger sliding distances. The specimen surfaces were all electropolished for about 15 minutes immediately before wear testing. The oil lubricated tests will be described first. The smallest sliding distance was 0.17 m (5 machine cycles). The contact along the track was reasonably uniform as shown in Fig. 4. A number of grains in and adjacent to the wear track were selected and SACP were obtained. Two of the

locations (A and D) on the surface in Fig. 4 produced the SACP shown in Fig. 5. The higher strains present in the track center lead to the lower contrast pattern seen in Fig. 5a. The strains determined from these SACP using the contrast-strain relation (Fig. 3) are plotted in Fig. 7 and will be discussed later. The grain configuration in this specimen is seen in Fig. 4 in the channeling contrast that results from grain orientation differences.

Two other sliding distances were studied, 1.7 and 17 m, under the same conditions in other respects. Figure 5a shows a portion of the wear track formed under oil lubricated conditions at the latter distance. The track is characterized by long, shallow groove markings in the sliding direction and by a lip of material at the track edge. Extensive plastic deformation has taken place in the surface material at the wear track. Adjacent to the track, slip lines can be seen in many of the grains (arrow, Fig. 5a). The amount of slip decreases rapidly with distance from the track edge. One test was conducted in which only a light film of oil was placed initially on the bearing pin contact. Under this limited lubrication condition the track appearance remained similar to that seen in Fig. 5a. The dry sliding tests produced a significantly different track appearance (Fig. 5b). The track was wider, more irregular and the groove markings within the track were much less prominant. The frictional coefficient over the last portion of the dry tests was typically 1.5, considerably higher than that found for oil lubricated tests of about 0.7. It is believed that a relatively "soft" loading pin suspension in the wear tester is responsible for some of the track features found, as a result of the higher frictional forces associated with the dry tests.

Strain Measurements

Shortly after each wear test was completed, SACP were obtained from the surface at various distances from the wear track center. A grain was selected that was sufficiently large, suitable in orientation and positioned across the track from which the SACP were obtained. At each location at least four values of contrast across the 111 band were obtained and averaged. The associated strain value was determined from the calibration curve (Fig. 3). The results are given in Fig. 7. A common feature of the lateral strain distribution is the rapid decrease in strain near and beyond the edge of the wear track. However, the surface strains still extend considerable distances

from the apparent edges of the wear tracks. For example, at a sliding distance of 17 m under oil, the strain at the track edge (70 μm) was about 24% and decreased to about 5% at twice that distance from the center. In two cases the strain could be measured over the entire track width and was found to increase steadily as the track center was approached. Since strains greater than about 36% could not be measured by the SACP method it was not possible to map out the entire surface distribution of strains in all cases. However, it appears that for sliding distances up to 17 m the maximum strain values at the surface are found at the track center position. Comparison of the 17 m sliding distance experiments under dry, oil film and oil bath conditions reveals that larger strains and a broader distribution are produced under dry conditions but otherwise the strain distribution is similar.

Measurements of the strain distribution with depth below the original surface were conducted after electropolishing for appropriate times to remove a specific thickness of material. The original track center could be located in all cases since the surface depression there persisted through the electropolishing steps. The results determined from three 17 m sliding distance experiments are shown in Fig. 8. In all cases the measured strains extend further lateral to the wear track than its edges (marked by arrow) even at subsurface locations. Within the track the maximum strains are found at the surface and decrease smoothly with depth, vanishing at depths of 50 μm or more depending on conditions. At any specific depth the maximum strain was found under the wear track center.

Relation to Other Studies

The strain measurement method described here has previously been applied to wear track deformation studies in iron (8). Qualitatively the results were similar in these two materials. The strain values in both materials decreased with depth below the worn surface and decreased with lateral distance from the wear track. At a given sliding distance, 17 m in oil, the strains in copper are about twice as large as in iron, both at the surface and at particular depths. The track center strains (50g, 17m) vanish at 30μm depth in iron and at about 50 μm depth in copper. Under dry conditions, the difference appears even greater. The surface slip

markings adjacent to the wear track in copper were more prominent than in iron, consistent with the evidence of more extensive plastic deformation.

Several previous studies of wear track material have been conducted in copper and similar metals. Some of those developed information that can be related to the results presented here. Bailey and Gwathmey (12) studied the effects of dry sliding wear on various orientations of copper single crystals. This included dislocation etch pit studies that demonstrated the rapid decrease in dislocation density with distance out from the wear track edge. Slip line observations adjacent to the tracks were consistent with those found here. They found considerable work hardening in the wear track and reported evidence of recrystallization when the deformation temperature reached 250 C. X-ray diffraction studies (averaged over 250 μm regions) of sliding on copper single crystals (13) revealed crystal plane bending and rotations resulting from slip deformation. The deformed layer was described as microsrystalline in structure. In another dry sliding study in copper (14) metallographic examination revealed evidence of recrystallization associated with the material below the worn (deformed) surface material. Microhardness measurements were conducted that showed decreases with distance from the wear surface that are consistent with the strain profiles found here. Other microhardness measurements have been reported for copper (15,16) involving material in and adjacent to sliding wear tracks that however, show some disagreement with respect to the trend of hardness values. Because of the influence of the free surface on hardness measurements (8) it is believed that quantitative comparisons may not be justified. Recently, Bill and Wisander (17,18) have reported wear track studies in copper under various conditions (including liquid methane environments where oxidation should be relatively slow). They found evidence for a small cell-sized recrystallized region near the wear surface in which the dislocations involved were predominantly located in the cell walls. The reported cell size of 5000A° was determined using transmission electron microscopy techniques on thin foils cut from the worn specimens. It is known from studies of the microstructure of plastically deformed copper that small cell sizes characterize relatively high levels of strain (19) and hence those results are consistent with the SACP broadening found here. Lacking a detailed theory of SACP broadening, it is not presently possible to distinguish uniform dislocation arrangements from cell-structure arrangements based on SACP data alone. Either possibility can be associated,

however, with the high level of deformation and hardening that is believed present.

The delamination model of wear (6) includes among other features the consideration of a "soft surface" region that forms during the wear deformation by the loss of dislocations through the free surface. The calculated depth of this region for copper was reported as about 10 μm although for the higher yield stress values usually associated with copper (4 MPa) a more representative figure would be 0.5 μm. The results reported here are not consistant with that picture, rather, they indicate a hardened layer at the surface and a decrease of strain with distance below the surface. The SACP are obtained from layers of material about 500 Å thick and about 10-15 μm in lateral dimensions. Thus the SACP obtained from the as-worn surface in copper are associated with the near-surface layer that is of interest in the delamination theory.

Detailed knowledge of the microstructure of the near surface region is being accumulated. Recent results (18) indicate that a transition in microstructure occurs below the worn surface. This microstructure transition may develop as a result of dynamic recrystallization processes that are driven by thermal and mechanical effects. If correct, that microstructure may alternatively satisfy the requirements for delamination processes that produce the wear debris particles frequently found.

SUMMARY

1) Strains up to 35% have been measured using a calibrated selected area electron channeling pattern method from wear track material in copper. Both the original surface and subsurface material were examined.

2) The maximum strains associated with the wear track material are always found at the surface and the track center. A soft or low dislocation density zone postulated by the delamination theory was not found in copper, nor in iron as previously reported.

3) The strain patterns developed in copper under dry and under lubricated conditions were similar; larger strain values were measured after dry sliding wear.

ACKNOWLEDGEMENTS

The work was partially supported by the Office of Naval Research and their interest is sincerely appreciated.

REFERENCES

1 Scott, D., "Debris Examination - A Prognostic Approach to Failure Prevention," Wear, Vol. 34, 1975, pp. 15-22.

2 Seifert, W. W., and Westcott, V. C., "A Method for the Study of Wear Particles in Lubricating Oil," Wear, Vol. 21, 1992

3 Ruff, A. W., "Characterization of Debris Particles Recovered from Wearing Systems," Wear, in press, 1976; see also NBS report 74-474, 1974.

4 Koba, H., and Cook, N. H., "Wear Particle Formation Mechanisms," ONR report NR229-003, 1974.

5 Scott, D., Seifert, W. W., and Westcott, V. C., "Ferrography - An Advanced Design Aid for the 80's" Wear, Vol. 34, 1975, pp. 251-260.

6 Suh, N. P., "The Delamination Theory of Wear," Wear, Vol. 25, 1973, pp. 111-124.

7 Suh, N. P., Jahanmir, S., Abrahamson, II, E. P., and Turner, A. P. L., "Further Investigation of the Delamination Theory of Wear," J. Lubr. Tech., Vol. 96, 1974, pp. 631-637.

8 Ruff, A. W., "Deformation Studies at Sliding Wear Tracks in Iron," Wear, 40, 59-74 (1976).

9 Stickler, R., Hughes, C. W., and Booker, G. R., "Application of the SA-ECD Method to Deformation Studies," SEM/1971, IITRI, 1971, pp. 473-480.

10 Spencer, J. P., Booker, G. R., Joy, D. C., and Humphreys, C. J., "Electron Channeling Patterns from Deformed Crystals," SEM/1974, IITRI, 1974, pp. 920-926.

11 Newbury, D. E., "The Origin, Detection and Uses of Electron Channelling Contrast," SEM/1974, IITRI, 1974, pp. 1047-1054.

12 Bailey, J. M., and Gwathmey, A. T., "Friction and Surface Deformation During Sliding on a Single Crystal of Copper," ASLE Trans., Vol. 5, 1962, pp. 45-56.

13 Roshon, Jr., D. D., "Selected Area X-ray Diffraction Studies of Surface Damage in Sliding on Single-Crystal Copper," J. Appl. Phys., Vol. 35, 1964, pp. 1262-1269.

14 Wibberley, R., and Eyre, T. S., "The Dry Sliding Wear Characteristics of Copper with and without 0.08% Silver," Wear, Vol. 13, 1969, pp. 27-38.

15 Tsuya, Y., "The Behavior of the Layer Damaged by Friction," Bull. Jap. Soc. Prec. Engg., Vol. 2, 1967, pp. 214-221.

16 Kirk, J. A., and Swanson, T. D., "Subsurface Effects During Sliding Wear," Wear, Vol. 35, 1975, pp. 63-67.

17 Bill, R. C., and Wisander, D. W., "Recrystallization as a Controlling Process in the Wear of some FCC Metals," preprint, 1976.

18 Bill, R. C., and Wisander, D. W., "Surface Recrystallization Theory of the Wear of Copper in Liquid Methane," NASA Technical Note TD D-7840, 1974.

19 Swann, P. R., "Dislocation Arrangements in Face-Centered Cubic Metals and Alloys," in Electron Microscopy and Strength of Crystals, Interscience, 1963, pp. 131-181.

FIGURE CAPTIONS

Fig. 1 Selected area channeling pattern from one grain in copper specimen. The 111 band is marked.

Fig. 2 SACP from grains in copper strain calibration specimen (a) C = 7.6%, ε = 5.0% (b) C = 2.3%, ε = 27%. The 111 bands are marked (arrows) and four signal traces are superimposed on each pattern.

Fig. 3 Strain vs. SACP contrast determined from calibration specimen.

Fig. 4 Portion of the wear track after 0.17 m sliding distance in oil. Locations of SACP obtained are marked.

Fig. 5 SACP from (a) location D and (b) location A in Fig. 4. Band of interest is marked.

Fig. 6 Wear tracks on specimens tested (a) in oil for 17 m sliding distance and (b) dry for 17 m. Locations at which SACP were obtained on original surface and below surface are marked.

Fig. 7 Strains determined for listed wear test conditions on original surface at various distances from track center.

Fig. 8 Strains determined for listed wear test conditions at indicated depths in specimens and various distances from track center.

Fig. 1 Selected area channeling pattern from one grain in copper specimen. The 111 band is marked.

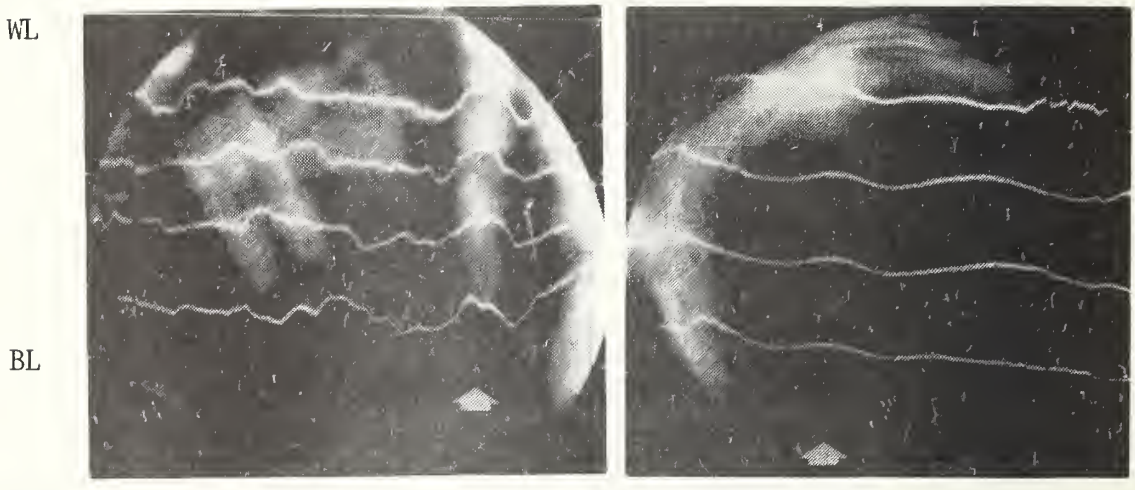

(a) (b)

Fig. 2 SACP from grains in copper strain calibration specimen (a) C = 7.6%, ε = 5.0% (b) C = 2.3%, ε = 27%. The 111 bands are marked (arrows) and four signal traces are superimposed on each pattern.

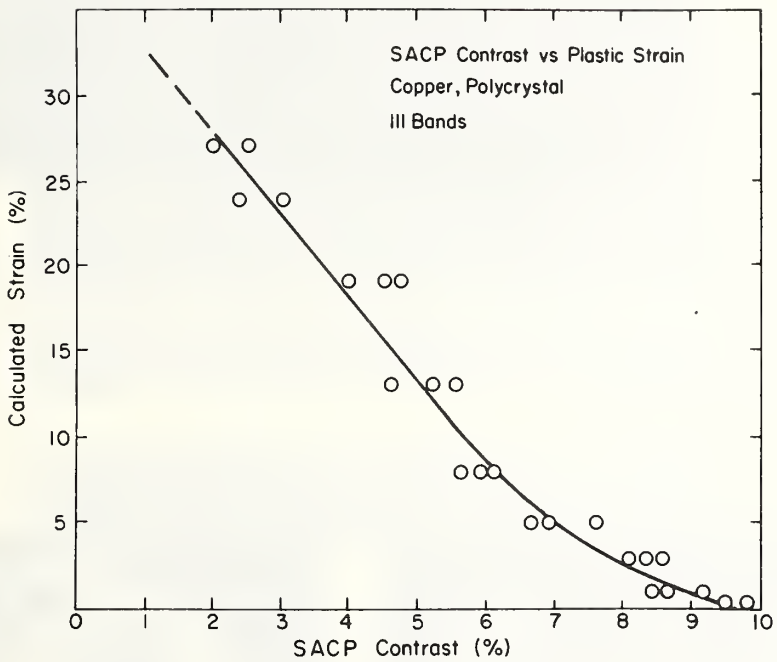

Fig. 3 Strain vs. SACP contrast determined from calibration specimen.

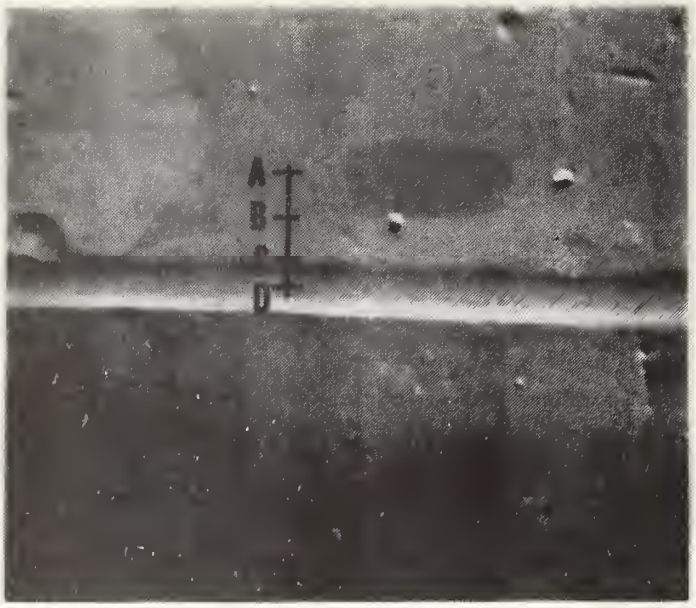

Fig. 4 Portion of the wear track after 0.17 m sliding distance in oil. Locations of SACP obtained are marked.

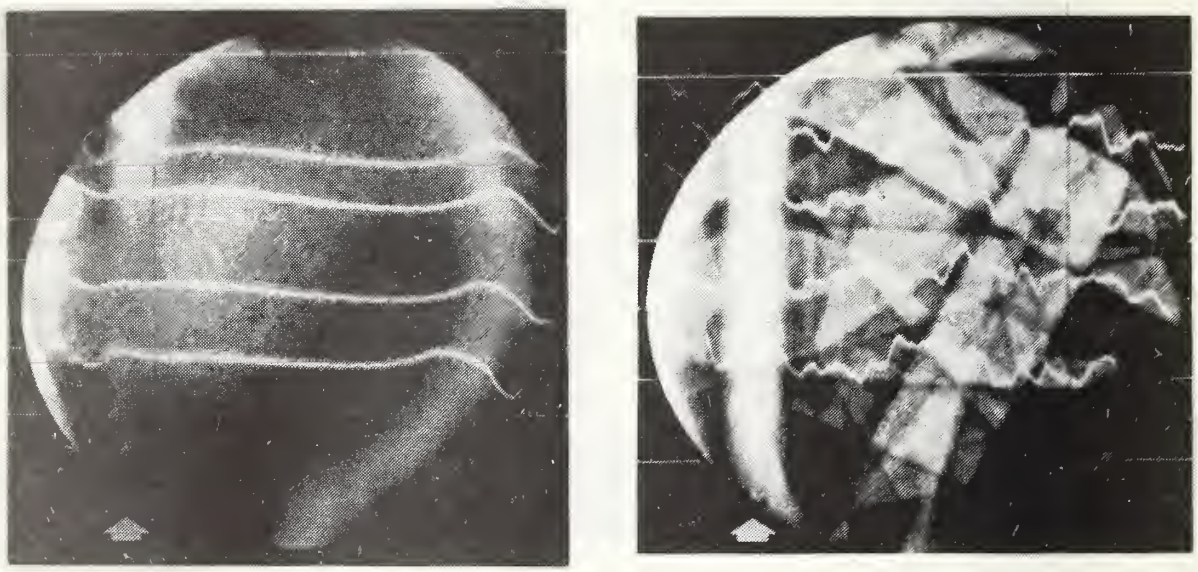

(a) (b)

Fig. 5 SACP from (a) location D and (b) location A in Fig. 4. Band of interest is marked.

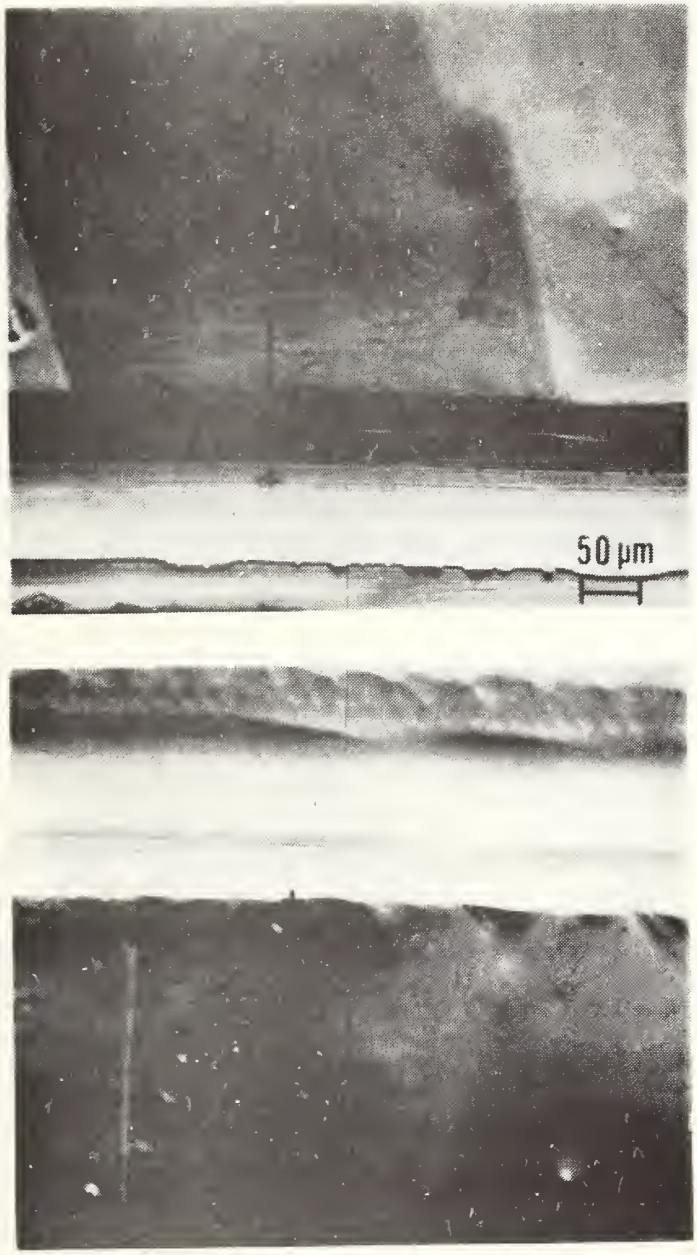

(a)

(b)

Fig. 6 Wear tracks on specimens tested (a) in oil for 17 m sliding distance and (b) dry for 17 m. Locations at which SACP were obtained on original surface and below surface are marked.

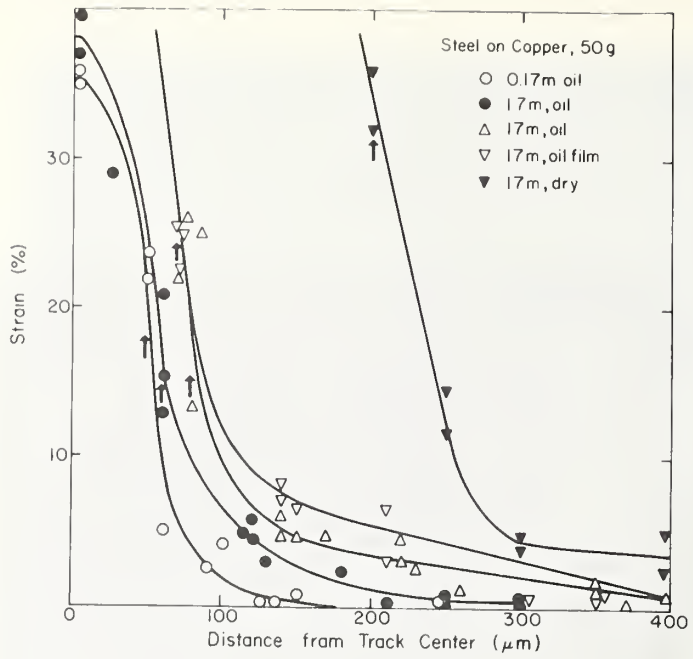

Fig. 7 Strains determined for listed wear test conditions on original surface at various distances from track center.

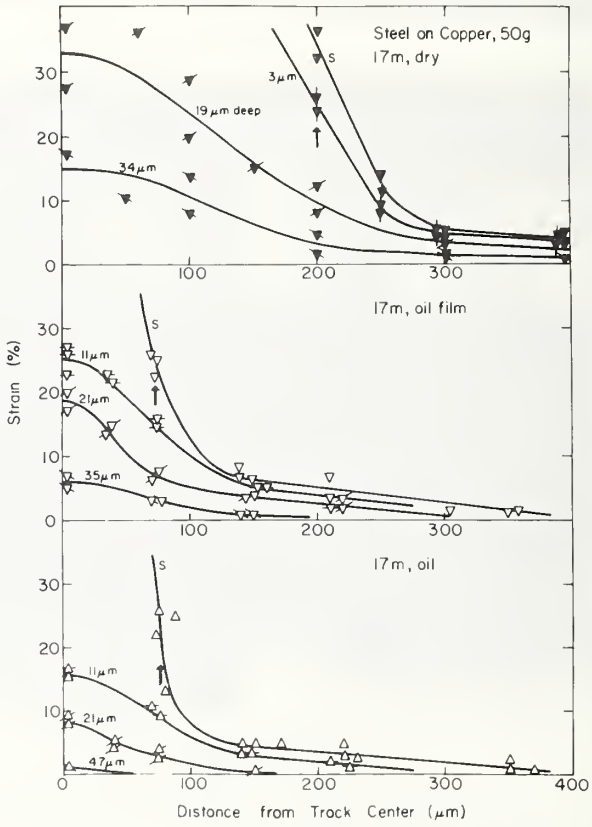

Fig. 8 Strains determined for listed wear test conditions at indicated depths in specimens and various distances from track center.

QUANTITATIVE METHODS IN WEAR DEBRIS ANALYSIS

A. W. Ruff
Metallurgy Division
National Bureau of Standards
Washington, D.C. 20234

ABSTRACT

Wear debris has been recovered from a number of test systems and analyzed using different methods. Those methods produced specific information concerning the particulate size and composition. A magnetic debris recovery method was quantitatively evaluated using actual debris samples and also using collections of manufactured particulates having known sizes and compositions. Small 5 μm diameter SiO_2 spheres, some containing nickel, were used to simulate debris. Other particulates of iron and nickel in different size ranges were also used in order to investigate such matters as size resolution, lubricant dilution techniques, particle overlap difficulties, and the general problem of calibration of debris recovery systems. A comparison between chemical analysis and particulate analysis findings is presented. The application of optical and electron microscope methods and X-ray microanalysis in characterizing the wear particulates was carried out directly on the recovery substrate; those techniques are described.

INTRODUCTION

The characterization of wear debris recovered from operating machines is frequently conducted for the purpose of evaluating the condition of the machine [1]. In that way, information additional to that obtained by chemical analysis of lubricants (SOAP) or through the monitoring of machine operating parameters can be acquired. Wear debris evaluation can also provide

insight into the operating mechanisms of wear, for example, distinguishing between adhesive wear and corrosive wear. In recent years, several detailed studies of wear debris have been reported [2-7]. In those cases, the authors have described useful techniques for debris recovery and analysis, and have contributed to an improved understanding of wear. While a few of the studies reported quantitative data determined from the debris analysis, much still remains to be done in that regard in order to place wear studies on a more quantitative basis. Progress in that direction will require development of more sophisticated (and accurate) measurement methods, including the means for calibrating those methods. This paper will describe several experiments involving quantitative comparisons of different debris analysis methods and some results using simulated debris collections.

EXPERIMENTAL

The wear debris and particulate collections studied here were recovered from lubricating oil by either of two methods. The first involved filtration through a perforated membrane filter (Nuclepore[1] type) with a pore diameter about 1 μm. That filter is characterized by a smooth, relatively structure-free surface that introduces a minimum of background detail during subsequent microscopic examination. After filtering the oil, naptha was passed through the filter to dissolve any remaining oil and wash the debris that was collected. The filter was then dried at 40 C in a vacuum oven for up to 1 hour, affixed to a specimen support stub and coated with a conductive layer of carbon in a vacuum evaporator. The debris could then be examined in place in a scanning electron microscope (SEM).

[1] Nuclepore Corporation. This item is identified here for the purpose of adequately describing the experimental method used in this study.

The second method utilized a magnetic separation process (Ferrography[2]) that passed a 2 ml volume of oil through a variable gradient magnetic field arranged so that the debris particles are deposited on a glass substrate. The particle location in the deposit depends on the particle magnetic moment (which in turn depends on its size and moment per unit volume). After preparation and washing in the recommended manner, the substrate was placed in a vacuum oven at 40 C for up to 1 hour. The substrate could then be coated with carbon for study in the SEM.

Examination in the SEM was conducted at 20 kV beam potential. Specimen currents ranged from 100 pA to 100 nA depending on the need to achieve sufficient x-ray emission intensity for analysis using the energy-dispersive x-ray detector system. In the x-ray studies, particles of interest were carefully oriented with respect to the detector in order to achieve good signal collection and avoid interference effects from neighboring particles.

The particulate collections reported on here consisted of wear debris samples recovered from turbine engine lubricants and bearing tests, and also several simulated collections. Porous silica microspheres were obtained[3] in two sizes, 5 μm and 0.7 μm average diameter. Some of the 5 μm spheres were impregnated with metallic nickel by chemically reducing an absorbed nickel complex. Iron powder particles of mean diameter 3 μm and nickel particles of 30 μm mean diameter were also used. Dispersions of the various particulates in automotive lubricating oil (SAE 30) were produced and then handled as actual oil-debris samples.

---

[2]Ferrograph, Foxboro/Trans-Sonics, Inc. These items are identified here for the purpose of adequately describing the experimental method used in this study.

[3]The silica sphere samples were provided through the kind cooperation of J. P. Wolf III and R. K. Iler, E. I. DuPont, Co.

RESULTS AND DISCUSSION

Silica Microspheres

A collection of the nickel-containing SiO_2 spheres is shown in Fig. 1. Some clustering on the Al substrate is seen as a result of evaporation of the liquid carrier. The size distribution of the spheres extends from about 3 μm to 7 μm with an average value of 5 μm. The uniformity of nickel content was determined by conducting x-ray microanalysis studies on a collection of spheres. The time required to accumulate 5000 counts of the Ni-Kα line was measured for each sphere in the collection. The average count time was 180 sec. with a standard deviation of 40 sec. The combination of size variation and nickel content variation thus roughly covered a range of ±50% about the mean value. This was felt to constitute a sufficiently narrow distribution for the present purpose of evaluating the debris recovery systems.

An oil sample containing a relatively dilute concentration of the Ni/SiO_2 spheres was passed through the magnetic recovery device. An optical micrograph of the resulting debris deposit is shown in Fig. 2a. The initial deposit volume is located at the upper position in the photograph. Below the initial deposit, the microspheres occur at a sharply reduced density. At a suitable concentration in the oil, a collection of uniformly sized spherical particles of the same composition would (ideally) be expected to all deposit in the initial volume. Some details on the particle configurations in the deposit are shown in Fig. 2b. The particle strings that form in the direction of the magnetic field lines start as a single row of the microspheres which increase in size by addition onto the ends. At some later stage particles attach at the side of the string to begin another row. After two

or more rows form in contact, a second layer can develop on top of the rows, thus thickening the deposit.

An equal volume mixture of SiO_2 and Ni/SiO_2 microspheres was prepared and added to clean oil in order to evaluate the magnetic recovery method with regard to non-metallic particles. The appearance of the deposit was essentially that seen in Fig. 2 in that very few SiO_2 spheres were deposited. Examination in transmitted light in the optical microscope revealed the non-nickel containing spheres since they transmit some light. The SiO_2 spheres were usually found at random locations on the substrate, not connected to the strings of nickel-containing spheres (Fig. 3). Clearly the magnetic recovery method cannot be used if reliable data on non-metallic particle fractions are desired.

Another mixture was prepared using equal volumes of 5 μm and 0.7 μm nickel-SiO_2 microspheres. An area on the magnetically recovered deposit is shown in Fig. 4, about 4 mm down from the entry deposit location. The 0.7 μm spheres are seen to deposit in groups of several spheres. That behavior probably results from some aglomeration of the spheres during preparation since single microspheres were rarely seen. Further down the deposit, the 0.7 μm microspheres predominated, still, however, in clustered units.

X-ray microanalysis studies were carried out on several particle strings in order to determine the uniformity of nickel content in particles of a particular string. One such group is shown in Fig. 5 and consists of both sizes of microspheres. The labeled particles were exposed to the incident electron beam in the SEM under nearly identical conditions of geometry, electron current density and electron spot size. The Ni-Kα x-ray results are shown in Table I.

Particles A, B and C are actually clusters of the smaller spheres. The variation in Ni count rate (proportional to Ni content) for the 5 μm spheres is due partly to statistical variation (about 6%) and partly to a real variation in Ni content. The average value of count time is 80 ± 18 sec; a variation of about 25%. The sample was rotated 180° in the SEM in order to reanalyze the end particles. The reanalyzed values (1R, 9R) are not significantly different from the original values indicating that electron excitation from adjacent particles was not a significant factor in producing the different count times for these two microspheres (numbers 1 and 9).

The effect of particle size and electron beam penetration on x-ray emission has previously been studied for iron - 3% silicon particles [7]. It was shown there that the x-ray emission intensity decreased rapidly for particle sizes below about 3 μm. That same size effect would be expected for nickel particles. Thus the size variation found among the 5 μm spheres does not require any correction, however, any comparison with the smaller 0.7 μm microspheres requires adjustment. The relative emission factor [7] at that size is about 0.3 so that the corrected count time values for clusters A and C is about (0.3) (350) = 100 sec. That value is reasonably consistent with the Ni-Kα count time values for the larger microspheres as given above.

Other Particulate Mixtures

A mixture of irregularly shaped 3 μm Fe particles and the 5 μm SiO_2 microspheres was prepared to further examine the differentiation of the magnetic recovery method for metallic and non-metallic mixtures. Equal volumes of the dry powders were added to clean lubricating oil. One sample was filtered through a 1 μm pore sized filter; the result is shown in Fig. 6a where the irregularly shaped particles are iron. The equi-volume initial proportion is consistant

with the appearance of this filter deposit. Another portion of the same oil sample was passed through the magnetic recovery system; the resulting deposit is shown in Fig. 6b. Only a very small fraction of non-metallic particles were recovered.

Another mixture of two types of metallic particulates consisted of an equal volume of 30 μm Ni particles and 3 μm Fe particles dispersed in lubricating oil. A deposit of that mixture that was magnetically recovered is shown in Fig. 7. The entry deposit region contained nearly all of the larger Ni particles (at the solids concentration used here), however, many of the smaller particles were also found at the entry volume. The smaller particles appear to deposit there as a result of locally high field strengths adjacent to the larger debris particles. Further down the deposit where the imposed magnetic field gradient is larger only the smaller 3 μm particles were found.

Oil Dilution Studies

The effect of different solids concentration in the oil on the quantitative recovery of debris was examined. In one experiment, a deposit of wear debris obtained from a jet engine lubrication system was recovered using the magnetic method. The deposit was characterized. It was then washed free from the substrate (using oil) and added to fresh oil of sufficient volume to obtain 1/5 the original concentration. That dilute sample was passed through the magnetic recovery system and analyzed with the results shown in Table II (the samples are designated K9 and 1/5:K9, respectively). The initial deposit height was measured using a calibrated fine focus control on an optical microscope. The initial deposit volume was calculated after microscopic

measurement. The relative area coverages were determined using photoelectric measurement of light transmission through the deposit at the indicated locations (measured from the initial deposit as origin). Those values do not represent absolute densities of the deposit. Examination of the results in Table II shows that the initial deposit volume ratio (6.6) and the coverage ratios (6.3 and 7.1) at the 1 mm and 5 mm location are comparable to the known debris concentration ratio (5.0). On the other hand, the initial deposit height and the relative coverage at the entry deposit do not change in proportion to the debris concentration and would be less satisfactory quantitative measures.

A second specimen was evaluated before and after a 10:1 dilution. The particulates in that set were 5 μm Ni/SiO_2 microspheres. As shown in Table II only the initial deposit volume ratio (11) and the area coverage ratio at 1 μm location (8.3) are comparable to the known particle concentration ratio (10). It is concluded that those two measures can be used with the most confidence in quantitative characterization of magnetically recovered debris.

Analytical Method Comparison

A sample of oil was obtained from a laboratory test of a tapered roller bearing. The sample was taken immediately prior to failure of that bearing. Spectrometric oil analysis readings had been obtained on this sample as well as on others periodically through the test duration. Wear debris samples had also been obtained periodically. The trends of those two measures of wear rate have been compared [8]; the interest here is with the last oil sample. The spectrometric reading was obtained at a SOAP

laboratory using conventional methods and indicated 6 ppm Fe. That same oil was further divided into two 1 g samples and analyzed here by wet chemical methods. That procedure indicated an iron content of 3.7 and 4.0 ppm, or an average of 3.8 ppm Fe. The spectrometric value is about 50% larger for this sample and appears to be inaccurate by that amount. Two other 2 ml samples were drawn from the same oil and passed through the magnetic recovery system to produce two debris deposits. The initial deposit volume was stripped from each slide using plastic replicating tape and subsequently analyzed by wet chemical methods. The two values obtained for iron particulate content in the initial deposit volume were 0.7 and 0.8 ppm Fe. The remaining debris particles on the slide (located below the initial deposit) were removed and found to total 0.8 and 1.1 ppm Fe. Thus the recovered debris particles totaled an average of 1.7 ppm Fe, with approximately 50% in the larger size group (3 to 50 μm, entry volume) and 50% in the smaller group (<2 μm). Clearly that ratio will depend on the debris size distribution and other factors. Of more interest here is the total particulate analysis of 1.7 ppm Fe which is only approximately 50% of the total iron content (3.8 ppm) found in the oil by analysis. Apparently, a large portion of the iron content occurs in extremely small particles that are not magnetically recovered or as a dissolved constituent. Further investigation is needed into this matter of wear product distribution within lubricants and into the comparison of methods of recovery and analysis.

SUMMARY

Experiments have been conducted on various types of actual and simulated wear debris particles recovered from lubricating oil using either filtration or magnetic deposition methods. Both spherical and randomly shaped particles were used in the size range 0.7 μm and 50 μm. The filter method cannot

discriminate between metallic and non-metallic particles. That feature is a disadvantage when the wear debris may be obscured by irrelevant contaminants such as carbon deposits, however, it would be an advantage in terms of recovering significant abrasives from the lubricant. The magnetic gradient method reliably recovers metallic debris and offers the advantage of additionally classifying the particles with regard to material type and size. That classification feature can probably be calibrated in a reasonably quantitative manner. The magnetic method cannot reliably recover non-metallic debris. Quantitative analysis methods can be carried out on the particle-substrate combination resulting from either method of debris recovery.

ACKNOWLEDGEMENTS

This work was partially supported by the Naval Air Engineering Center, Lakehurst, New Jersey. The contribution of oil samples and valuable information and discussion by H. Dalal, V. Westcott and co-workers is gratefully acknowledged.

Particles	1	2	3	4	5	6	7	8	9	A	B	C	1R	9R
Time for 10^3 counts (sec.)	108	87	79	70	77	104	76	60	58	350	112	360	99	53

Table I. X-ray microanalysis results on particles identified in Fig. 5.

Sample	Initial Deposit		Relative Area Coverage at Indicated Location		
	Volume (μm^3)	Height (μm)	Entry	1mm	5mm
K9	6.6×10^6	65	36	14	5
1/5:K9*	1.0×10^6	24	11	2.2	0.7
ratio	6.6	2.8	3.3	6.3	7.1
NBS-7	1.2×10^6	23	14	5	0.6
1/10:NBS-7	0.11×10^6	12	2.5	0.6	---
ratio	11	2.0	5.6	8.3	---

*Particles were washed from original deposit.

Table II. Magnetic Recovery System - Dilution Effects on Performance

FIGURE CAPTIONS

Fig. 1 - Nickel-containing SiO_2 microspheres; average diameter 5 μm.

Fig. 2 - Deposit of nickel-containing SiO_2 spheres. (a) Initial deposit at upper end. (b) Details of particle arrangements in groups.

Fig. 3 - Equal volume mixture of 5 μm SiO_2 spheres and Ni/SiO_2 spheres after magnetic separation. Details near edge of deposit. SiO_2 spheres are marked.

Fig. 4 - Group of particles from mixture of 5 μm and 0.7 μm Ni/SiO_2 spheres.

Fig. 5 - Group of 0.7 μm and 5 μm Ni/SiO_2 spheres used in x-ray micro-analysis study.

Fig. 6 - (a) Oil sample containing equal volume mixture of 5 μm SiO_2 spheres and 3 μm Fe particles, filtered through 1 μm pore sized filter. (b) Magnetic separation deposit from above mixture. Four SiO_2 spheres are seen in this region.

Fig. 7 - Magnetic separation deposit of a mixture of 30 μm Ni particles and 3 μm Fe particles. Entry deposit region contains all large particles and some small particles.

REFERENCES

1. Scott, D., "Debris Examination - A Prognostic Approach to Failure Prevention," Wear 34 (1975) 15-22.

2. Seifert, W. W., and Westcott, V. C., "A Method for the Study of Wear Particles in Lubricating Oil," Wear 21 (1972) 27-42.

3. Westcott, V. C., and Seifert, W. W., "Investigation of Iron Content of Lubricating Oil using a Ferrograph and an Emission Spectrometer," Wear 23 (1973) 239-249.

4. Koba, H., and Cook, N. H., "Wear Particle Formation Mechanisms," ONR report NR229-003 (1974).

5. Jones, W. R., "Ferrographic Analysis of Wear Debris from Boundary Lubrication Experiments with Five Ring Polyphenylether," ASLE Trans. 18 (1975) 153-162.

6. Scott, D., Seifert, W. W., and Westcott, V. C., "Ferrography - An Advanced Design Aid for the 80's," Wear 34 (1975) 251-260.

7. Ruff, A. W., "Characterization of Debris Particles Recovered from Wearing Systems," Wear, in press (1976); see also NBS report 74-474 (1974).

8. Westcott, V. C., private communication.

Fig. 1. Nickel-containing SiO_2 microspheres; average diameter $5^2\mu m$

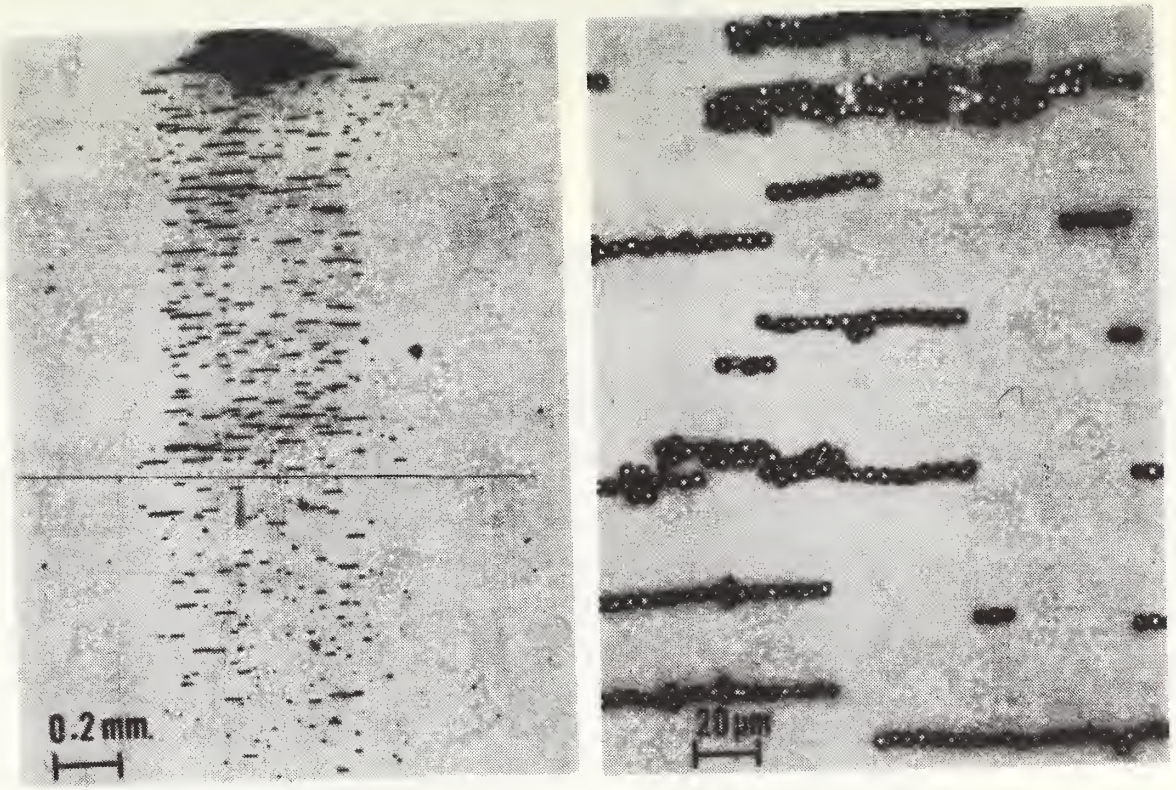

Fig. 2. Deposit of nickel-containing SiO_2 spheres.
(a) Initial deposit at upper end.
(b) Details of particle arrangements in groups.

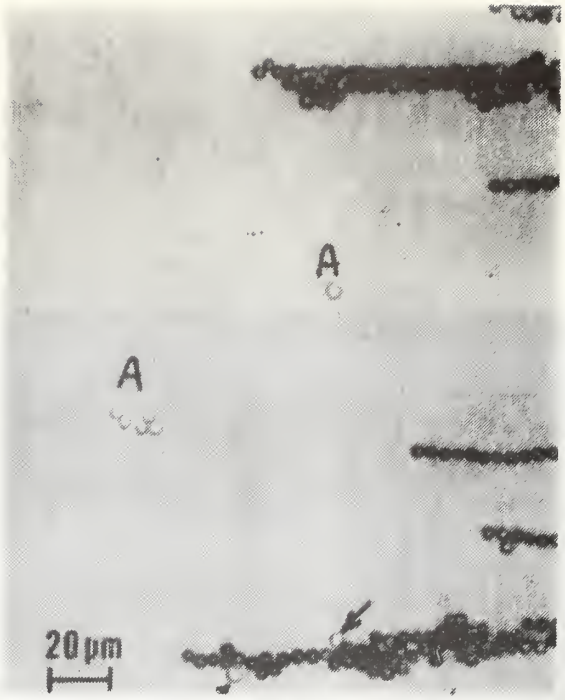

Fig. 3. Equal volume mixture of 5 µm SiO_2 spheres and Ni/SiO_2 spheres after magnetic separation. Details near edge of deposit. SiO_2 spheres are marked.

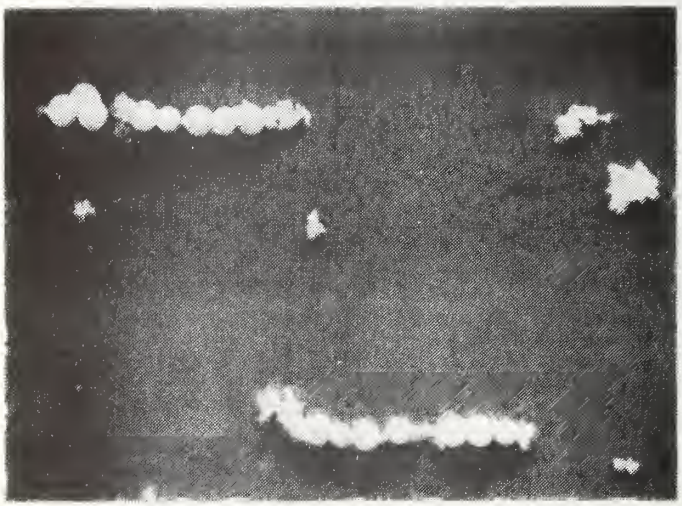

Fig. 4. Group of particles from mixture of 5 µm and 0.7 µm Ni/SiO_2 spheres.

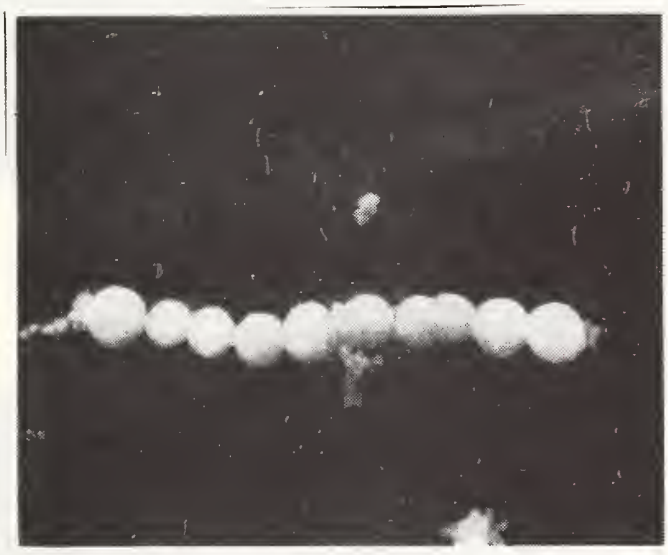

Fig. 5. Group of 0.7 μm and 5 μm Ni/SiO_2 spheres used in x-ray microanalysis study.

Fig. 6. (a) Oil sample containing equal volume mixture of 5 μm SiO_2 spheres and 3 μm Fe particles, filtered through 1 μm pore sized filter.

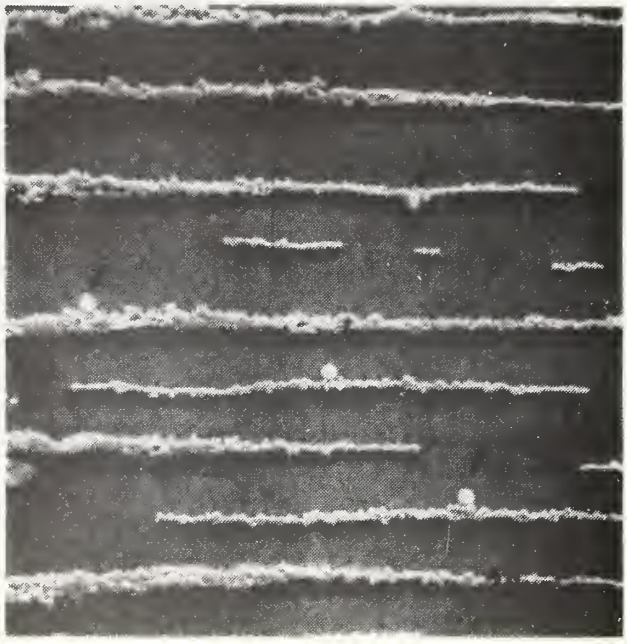

(b) Magnetic separation deposit from above mixture. Four SiO_2 spheres are seen in this region.

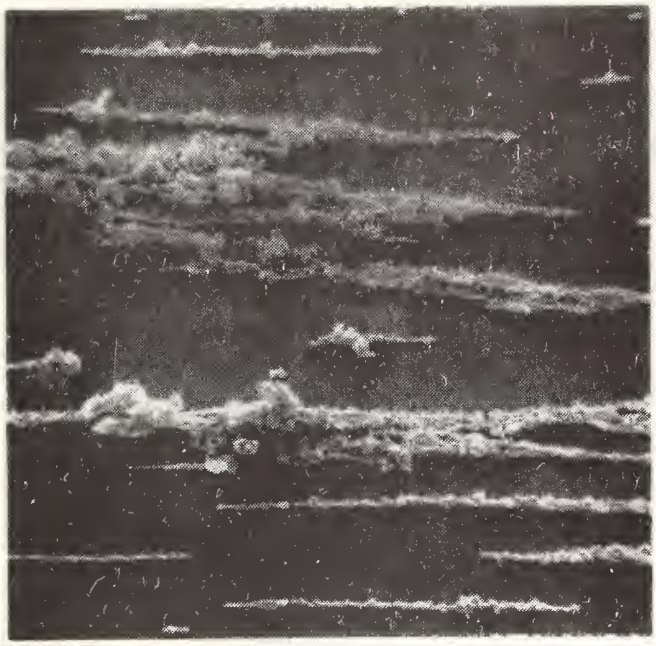

Fig. 7. Magnetic separation deposit of a mixture of 30 μm Ni particles and 3 μm Fe particles. Entry deposit region contains all large particles and some small particles.

DISTRIBUTION LIST

	NO. OF COPIES
Office of Naval Research Arlington, Virginia 22217 Attn: Code 211, R.S. Miller, K.Petrovic	2
Office of Naval Research Contract Administrator, Southeastern Area 2110 G Street, N.W. Washington, D.C. 20037	1
Director Naval Research Laboratory Washington, D.C. 20375 Attn: Technical Information Division Code 2029	6
Defense Documentation Center Building 5 Cameron Station Alexandria, Virginia 22314	12
Air Force Materials Lab Wright-Patterson Air Force Base Dayton, Ohio 45433 Attn: Mr. F. Brooks	1
Department of Mechanical Engineering University of Virginia Charlottesville, Virginia 22091 Attn: P. Allaire	1
Department of Mechanical Engineering Chico State College Chico, California 95926 Attn: C. W. Allen	1
NASA-Lewis Research Center 21000 Brookpark Road Cleveland, Ohio 44135 Attn: W. J. Anderson	1
U.S. Steel Corporation Applied Research Lab Mailing Station 63 Monroeville, Pa. 15146 Attn: C. A. Bailey	1
Esso Research and Engineering Co. P. O. Box 51 Linden, New Jersey 07036 Attn: A. Beerbower	1

Mechanical Engineering Department
Massachusetts Institute of Technology
Cambridge, Mass. 02139
Attn: B. G. Bightmire 1

E. E. Bisson
20786 Eastwood Avenue
Fairview Park, Ohio 44126 1

Sibley School of Mechanical Engineering
Cornell University
Ithaca, New York 14350
Attn: J. E. Booker 1

Westinghouse Research Labs
Beulah Road
Churchill Boro
Pittsburgh, Pa. 15235
Attn: P. H. Bowen 1

Department of Mechanical Engineering
Georgia Institute of Technology
Atlanta, Georgia 30332
Attn: J. M. Bradford 1

General Electric Company
Silicon Products Department
Waterford, New York 12188
Attn: E. D. Brown, Jr. 1

Naval Research Laboratory
Washington, D.C. 20375
Attn: R. C. Bowers, Code 6050 1

NASA-Lewis Research Center
21000 Brookpark Road
Cleveland, Ohio 44135
Attn: D. A. Buckley 1

Department of Mechanical Engineering
and Astronautical Sciences
Northwestern University
Evanston, Illinois 60201
Attn: H. S. Cheng 1

Wear Sciences Inc.
32 Sutherland Drive
Scotia, New York 12302
Attn: W. Campbell 1

Xerox Corporation
701 S. Aviation
El Segundo, California 90245
Attn: S. Chai 1

Department of Mechanical Engineering
and Astronautical Sciences
Northwestern University
Evanston, Illinois 60201
Attn: R. A. Burton 1

Institute of Fluid Mechanics
Academy of the Socialist Republic Rumania
Bucharest, Rumania
Attn: V. M. Constantinescu 1

John Deere Waterloo Tractor Works
Waterloo, Iowa 50704
Attn: P. K. Das 1

Aero Material Department
Naval Air Development Center
Johnsville, Warminster, PA 18974
Attn: M. J. Devine 1

Office of Naval Research
Arlingtin, Virginia 22217
Attn: S. Doroff 1

Virginia Polytechnic Institute
Blacksburg, Virginia 24060
Attn: N. S. Eiss, Jr. 1

Department of Mechanical Engineering
Columbia University
New York, New York 10027
Attn: H. G. Elrod 1

IBM Corporation
Systems Products Division
Endicott, New York 13760
Attn: P. A. Engel 1

Fundamental Research Section
Research and Technical Department
Texaco Research Center
Beacon, New York 12508
Attn: R. Fein 1

Mechanical Engineering Department
Virginia Polytechnic and State University
Blacksburg, Virginia 24060
Attn: M. Furey 1

Naval Air Development Center
Johnsville, Warminster, PA 18974
Attn: M. K. Gabel 1

Chevron Research Company
576 Standard Avenue
Richmond, California 94800
Attn: D. Godfrey 1

Department of Mechanical Engineering
University of Virginia
Charlottesville, VA 22091
Attn: E. J. Gunter 1

Mechanical Development Department
Research Laboratories
General Motors Corporation
Warren, Michigan 48090
Attn: D. F. Hays 1

Department of Machine Design
Technical University of Denmark
DK 2800 Lyngby, Denmark
Attn: J. Jakobsen 1

Department of Mechanical Engineering
University of Virginia
Charlottesville, VA 22091
Attn: W. Jamaison 1

NASA-Lewis Research Center
21000 Brookpark Road
Cleveland, Ohio 44135
Attn: R. L. Johnson 1

University of Virginia
Thornton Hall
Charlottesville, VA 22091
Attn: J. J. Kauzlarich 1

Cincinnati, Inc.
P. O. Box 11111
Cincinnati, Ohio 45211
Attn: R. A. Ketterer 1

Mechanical Engineering Department
Texas A&H University
College Station, Texas 77840
Attn: D. F. Kettlebourgh 1

Department of Chemical Engineering
Pennsylvania State University
University Park, PA 16802
Attn: E. E. Klaus 1

Director, Department of Aerospace
Properties Research
Southwest Research Institute
8500 Culebra Road
San Antonio, Texas 78206
Attn: P. M. Ku 1

Department of Mechanical Engineering
Cleveland State College
Cleveland, Ohio 44115
Attn: V. H. Larson 1

Department of Mechanics
Rensselaer Polytechnic Institute
Troy, New York 12181
Attn: F. F. Ling 1

Timken Company
1835 Dueber Avenue, S.W.
Canton, Ohio 44706
Attn: W. E. Littmann 1

Department of Mechanical Engineering
University of Michigan
Ann Arbor, Michigan 48105
Attn: K. Ludema 1

Department of Engineering Mechanics
North Carolina State University
Raleigh, N.C. 27607
Attn: C. J. Maday 1

Ford Motor Company
Research Laboratory
Dearborn, Michigan 48120
Attn: J. Meyer 1

Mobil Research & Development Corp.
Central Research Division
Box 1025
Princeton, N.J. 08540
Attn: W. R. Murphy 1

National Science Foundation
Engineering Mechanics Division
1800 G Street
Washington, D.C. 20550
Attn: M. S. Ojalvo 1

Shaker Research, Inc.
Latham, New York 12110
Attn: C. T. Pan 1

NASA-Lewis Research Center
21000 Brookpark Road
Cleveland, Ohio 44135
Attn: R. Parker 1

Wear Sciences, Inc.
32 Sutherland Drive
Scotia, New York 12302
Attn: M. B. Peterson 1

Mechanical Engineering Department
Cornell University
Ithaca, New York 15850
Attn: R. M. Phelan 1

Mobil Research and Development Corp.
Box 1025
Princeton, New Jersey 08540
Attn: C. N. Rowe 1

Department of Mechanical Engineering
Georgia Institute of Technology
Atlanta, Georgia 30332
Attn: D. M. Sanborn 1

Department of Materials Engineering
University of Illinois at Chicago Circle
Box 4348
Chicago, Illinois 60680
Attn: J. A. Schey 1

University of Wisconsin
1513 University Avenue
Madison, Wisconsin 53706
Attn: A. Seireg 1

Mechanical Engineering Deparment
Carnegie-Mellon University
Pittsburgh, PA 15213
Attn: M. C. Shaw 1

Maic Division
Pure Carbon Co., Inc.
St. Mary's, PA 15857
Attn: J. J. Sherlock 1

Pratt & Whitney Aircraft (MS-EB2B)
400 Main Street
East Hartford, Conn.
Attn: R. P. Sevchenko 1

SKF Industries, Inc.
1100 First Avenue
King of Prussia, PA 15857
Attn: L. B. Sibley 1

Mechanical Engineering Department
University of Tennessee
Knoxville, Tennessee 37916
Attn: K. Stair 1

Ford Motor Company
Research Laboratory
Dearborn, Michigan 48120
Attn: L. Ting 1

General Electric Company
Building 55-119
Schenectady, New York 12305
Attn: J. H. Vohr 1

Manager, Bearings, Lubrication & Seals
Mechanical Technology, Inc.
968 Albany Shaker Road
Latham, New York 12110
Attn: D. F. Wilcock 1

Department of Mechanical Engineering
Georgia Institute of Technology
Atlanta, Georgia 30332
Attn: W. O. Winer 1

NASA-Lewis Research Center
21000 Brookpark Road
Cleveland, Ohio 44135
Attn: E. V. Zaretsky 1

Office of Naval Research
Arlington, Virginia 22217
Attn: P. Clarkin, Code 471 1
K. Ellingsworth, Code 473 1

Naval Ship Engineering Center
Prince George's Center
Hyattsville, Maryland 20782
Attn: L. B. Hebbard, Code 6107 1
R. Lane, Code 6101F 1

Naval Air Systems Command
Washington, D.C. 20360
Attn: B. Poppert, Code 340E 1
E. Regelson, Code 4115 1
H. Rosenwasser, Code 424 1

Chief, of Naval Material
Washington, D.C. 20360
Attn: CAPT W. Holton, Code 041 1
CAPT G. D. Webber, Code 09H 1
J. Ward, 04112 1

Naval Air Engineering Center
Ground Support, Equipment Division
Philadelphia, PA 19112
Attn: Code SE-624, P. Senholze 1

Naval Ship Research & Development Lab.
Annapolis, Maryland 21401
Attn: Mr. N. Glassman, Code 821 1
Mr. W. Smith, Code 2832 1

Air Force Aero Propulsion Laboratory
AFAPL/SFL
Wright Patterson Air Force Base, Ohio 45433
Attn: Mr. C. Hudson 1

National Engineering Laboratory
East Kilbridge, Glasgow (G. Britain)
Attn: Mr. D. Scott 1

National Bureau of Standards
Department of Commerce
Washington, D.C. 20234
Attn: Dr. E. Passaglia 1
Dr. A. W. Ruff 1

Institute of Ocean Science & Engineering
Dept. of Civil & Mechanical Engineering
The Catholic University of America
Washington, D.C. 20017
Attn: Dr. A. Thiruvengadam 1

U.S. Army Mobility Equipment Command
Directorate of Research, Development & Engineering
Fort Belvoir, Virginia 22060
Attn: Mr. A. J. Rutherford 1

Office of Secretary of Defense (I&L)
The Pentagon, Room 2B322
Washington, D.C. 20350
Attn: Mr. H. Peterson 1

AFSME Oil Analysis Section
Room 4A264, The Pentagon
Washington, D.C. 20350
Attn: COL Benjamin 1

University College of Swansea
Singleton Par.
Swansea, Wales SA28PP
Attn: Prof. F. T. Barwell 1

Massachusetts Institute of Technology
Lincoln Laboratory
Cambridge, Mass 02139
Attn: Prof. N. Cook 1
Prof. E. Rabinowicz 1
Prof. N. Suh 1

Imperial College of Science & Technology
Dept. of Mechanical Engineering
Exhibition Road
London, England SW7
Attn: Prof. Alistair Cameron 1

AB-SVENSKA KULLAGERFABRIKEN
Group Headquarters
S-41550
Gothenberg, Sweden
Attn: Dr. A. Palmgren 1

Mr. Robert Q. Barr
Associate Director
Technical Information
Climax Molybdenum Company
1270 Avenue of Americas
New York, New York 10020 1

Commander
Naval Ships Systems Command
Code 045N
Washington, D.C. 20362 1

Naval Ordance Systems Command
Code 0442
Washington, D.C. 20360
Attn: G. Tsuchida 1

Naval Ordance Systems Command
Code ORD-04531
Washington, D.C. 20360
Attn: A. R. Romano 1

Naval Ordance Systems Command
Washington, D.C. 20360
Attn: CDR F. Jonasz 1

Naval Ordnance Station
Code 50331
Louisville, Kentucky 40214
Attn: J. W. Patton 1

Quality Evaluation & Engineering Laboratory
NAD/Oahu (Code 3032)
FPO San Francisco 96612
Attn: Seiji Sakata 1

Commander Cruiser Destroyer Force
Atlantic Fleet
Code 414
Norfolk, Virginia 23511
Attn: FTCS Buchanan 1

Commander
Cruiser Destroyer Force
Pacific Fleet
Code 434
San Diego, California 92110
Attn: Chief Collins 1

Commanding Officer
Naval Ordnance Systems Support Office, Atlantic
Building #62
Norfolk Naval Shipyard
Portsmouth, VA 23709
Attn: J. Reidy 1

Commanding Officer
Naval Ordnance Systems Support Office, Pacific
Post Office Box 80548
San Diego, California 92138
Attn: Code 081 Clay Westfall 1

Commanding Officer
Naval Ship Engineering Center
Code 6101F
Prince George's Center
Hyattsville, Maryland 20782
Attn: E. C. Davis 1

Commanding Officer
Naval Air Rework Facility
Technical Support Center (Code 360)
Naval Air Station
Pensacola, FLA 32508
Attn: R. Purcell 1

Commander
Charleston Naval Shipyard
Metals Section
Material Laboratory (Code 134.11)
Charleston, S.C. 29408
Attn: Hillary Douglas 1

Commander
Naval Ship Repair Facility
Subic
FPO San Francisco 96612 1

Commander
Naval Ship Repair Facility
Guam
FPO San Francisco 96612 1

Department of Chemistry
University of North Carolina
Chapel Hill, N.C. 27514
Attn: Dr. T. Isenhower 1

Assistant Chief for Technology
Office of Naval Research, Code 200
Arlington, Virginia 22217 1

Prof. R. M. Latanision
Metallurgy Dept., 8-202
MIT
Cambridge, Mass. 02139 1

Mr. V. C. Westcott
Trans Sonics, Inc.
P. O. Box 326
Lexington, Massachusetts 02713 1

Dr. Ranga Komanduri
Carnegie-Mellon University
Mechanical Engineering
Pittsburgh, PA 15213 1

Dr. Robert I. Jaffee
Technical Manager, Materials
Electric Power Research Institute
3412 Hillview Avenue
P. O. Box 10412
Palo Alto, CA 94304 1

Dr. Bernard H. Kear
Materials Engineering and Research Laboratory
Pratt & Whitney Aircraft
Middletown Plant
Middletown, Connecticut 06457 1

Dr. F. S. Pettit
Materials Engineering & Research Laboratory
Pratt & Whitney Aircraft
Middletown Plant
Middletown, Connecticut 06457 — 1

Dr. B. A. Wilcox
Division of Materials Research
National Science Foundation
1800 G Street
Washington, D.C. 20550 — 1

Dr. I. G. Wright
Metal Science Section
Battelle Columbus Laboratories
505 King Avenue
Columbus, Ohio 43201 — 1

Prof. I. Finnie
Dept. of Mechanical Engineering
University of California
Berkeley, CA 94720 — 1

Dr. Edward Van Reuth
ARPA
1400 Wilson Blvd
Arlington, VA 22209 — 1

Dr. E. Saibel
Army Research Office
P. O. Box 1221
RTP, North Carolina 27709 — 1

Prof. David A. Rigney
Dept. of Metallurgical Engineering
The Ohio State University
116 West 19th Avenue
Columbus, Ohio 43210 — 1

NBS-114A (REV. 7-73)

U.S. DEPT. OF COMM. BIBLIOGRAPHIC DATA SHEET	1. PUBLICATION OR REPORT NO. NBSIR - 1141	2. Gov't Accession No.	3. Recipient's Accession No. AD AO 31530

4. TITLE AND SUBTITLE

Study of Initial Stages of Wear by Electron Channeling
I. Measurement of Plastic Strain in Copper Due to Sliding Wear
II. Quantitative Methods in Wear Debris Analysis

5. Publication Date: October 1976

6. Performing Organization Code

7. AUTHOR(S): A. W. Ruff

8. Performing Organ. Report No.

9. PERFORMING ORGANIZATION NAME AND ADDRESS

NATIONAL BUREAU OF STANDARDS
DEPARTMENT OF COMMERCE
WASHINGTON, D.C. 20234

10. Project/Task/Work Unit No. 3120438

11. Contract/Grant No. N00014-76-F-002

12. Sponsoring Organization Name and Complete Address (*Street, City, State, ZIP*)

Department of the Navy
Office of Naval Research
Arlington, VA 22217

13. Type of Report & Period Covered: Final Report

14. Sponsoring Agency Code

15. SUPPLEMENTARY NOTES

16. ABSTRACT (*A 200-word or less factual summary of most significant information. If document includes a significant bibliography or literature survey, mention it here.*)

Wear experiments have been conducted to determine the plastic strains that are introduced in the surface material near sliding wear tracks. Both oil lubricated and dry sliding experiments have been carried out at different sliding distances on surfaces of copper. The strain values were determined from selected area electron channeling patterns obtained using a scanning electron microscope from regions as small as 10 μm in size and 0.05 μm deep around the wear track. A deformed calibration specimen was used to relate electron channeling band contrast to deformation strain. Strain maps were obtained on the wear surface lateral to the wear track and also below the surface using electropolishing metal removal techniques. Particular attention was placed on the near-surface strain values. In all cases, the maximum strain was found at the wear surface located at the track center and the strains decreased uniformly with depth. Significant, large strains were also found outside the wear tracks. The results are compared with those previously reported for iron and with recent theoretical models.

Wear debris has been removed from a number of test systems and analyzed using different methods. Those methods produced specific information concerning the particulate size and composition. A magnetic debris recovery method was quantitatively evaluated using actual debris samples and also using collections of manufactured

(CONTINUED ON ATTACHED)

17. KEY WORDS (*six to twelve entries; alphabetical order; capitalize only the first letter of the first key word unless a proper name; separated by semicolons*)

Copper; electron channeling; electron microscope; metals; particle analysis; plastic deformation; surfaces; wear; wear debris; x-ray analysis.

18. AVAILABILITY

[XX] Unlimited

[ ] For Official Distribution. Do Not Release to NTIS

[ ] Order From Sup. of Doc., U.S. Government Printing Office Washington, D.C. 20402, SD Cat. No. C13

[ ] Order From National Technical Information Service (NTIS) Springfield, Virginia 22151

19. SECURITY CLASS (THIS REPORT)	21. NO. OF PAGES
UNCLASSIFIED	
20. SECURITY CLASS (THIS PAGE)	22. Price
UNCLASSIFIED	

USCOMM-DC 29042-P74

NBS-114A (REV. 7-73)

U.S. DEPT. OF COMM. BIBLIOGRAPHIC DATA SHEET	1. PUBLICATION OR REPORT NO. NBSIR-1141 Continued	2. Gov't Accession No.	3. Recipient's Accession No. AD AO 31530
4. TITLE AND SUBTITLE			5. Publication Date
			6. Performing Organization Code
7. AUTHOR(S)			8. Performing Organ. Report No.
9. PERFORMING ORGANIZATION NAME AND ADDRESS NATIONAL BUREAU OF STANDARDS DEPARTMENT OF COMMERCE WASHINGTON, D.C. 20234			10. Project/Task/Work Unit No. 11. Contract/Grant No.
12. Sponsoring Organization Name and Complete Address (*Street, City, State, ZIP*)			13. Type of Report & Period Covered 14. Sponsoring Agency Code
15. SUPPLEMENTARY NOTES			

16. ABSTRACT (*A 200-word or less factual summary of most significant information. If document includes a significant bibliography or literature survey, mention it here.*)

particulates having known sizes and compositions. Small 5 μm diameter SiO_2 spheres, some containing nickel, were used to simulate debris. Other particulates of iron and nickel in different size ranges were also used in order to investigate such matters as size resolution, lubricant dilution techniques, particle overlap difficulties, and the general problem of calibration of debris recovery systems. A comparison between chemical analysis and particulate analysis findings is presented. The application of optical and electron microscope methods and x-ray microanalysis in characterizing the wear particulates was carried out directly on the recovery substrate; those techniques are described.

17. KEY WORDS (*six to twelve entries; alphabetical order; capitalize only the first letter of the first key word unless a proper name; separated by semicolons*)

18. AVAILABILITY	19. SECURITY CLASS (THIS REPORT)	21. NO. OF PAGES
☒ Unlimited ☐ For Official Distribution. Do Not Release to NTIS ☐ Order From Sup. of Doc., U.S. Government Printing Office Washington, D.C. 20402, SD Cat. No. C13 ☐ Order From National Technical Information Service (NTIS) Springfield, Virginia 22151	UNCLASSIFIED	
	20. SECURITY CLASS (THIS PAGE) UNCLASSIFIED	22. Price

USCOMM-DC 29042-P74